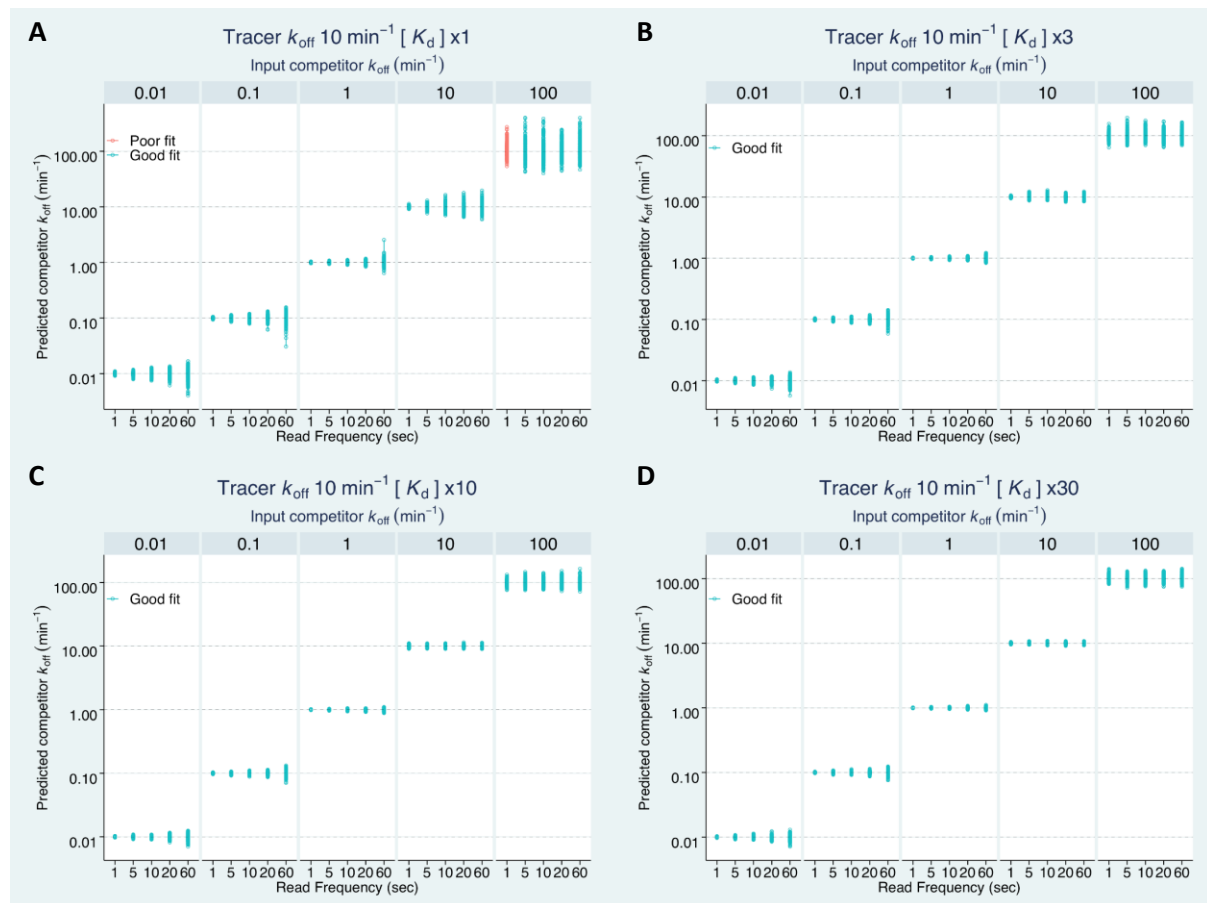


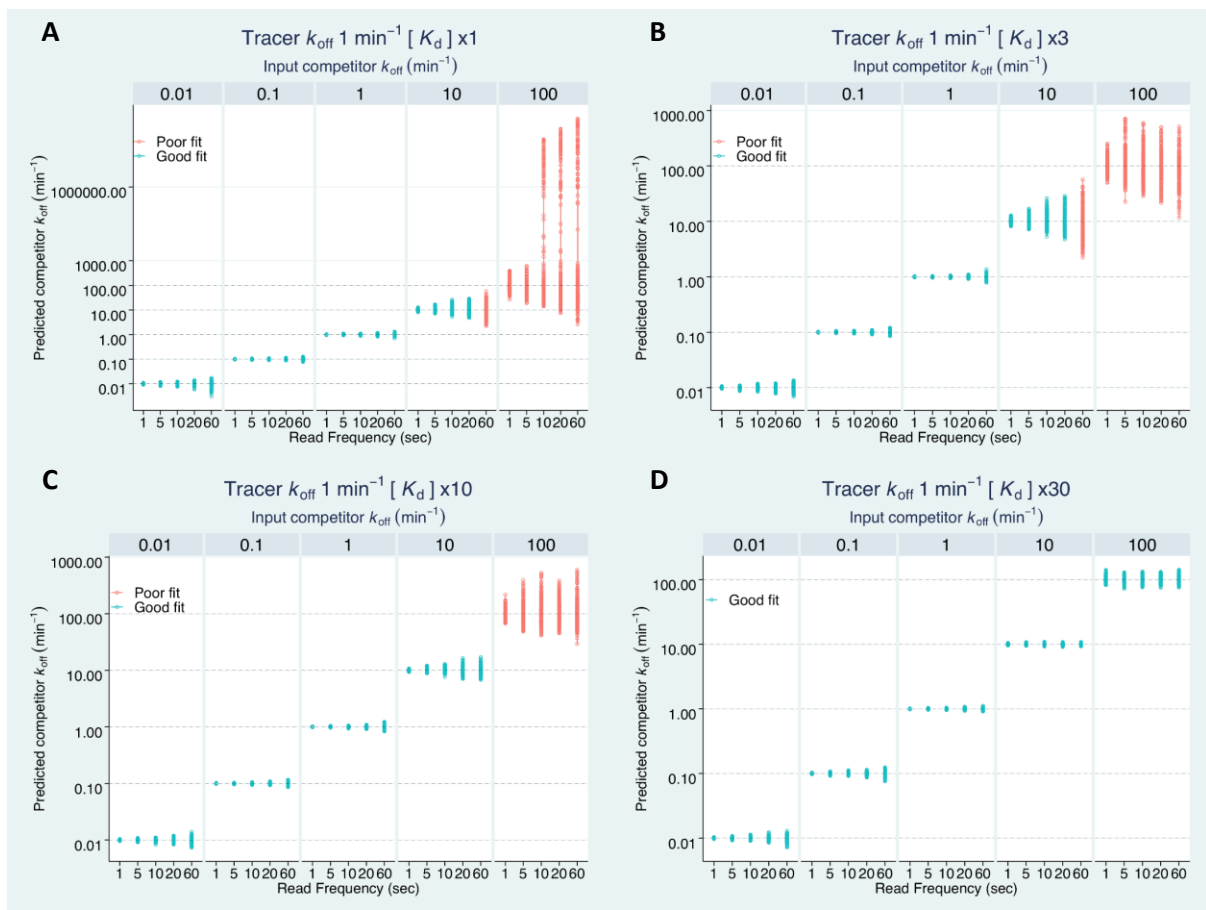
Investigating the influence of tracer kinetics on competition-kinetic association binding assays; identifying the optimal conditions for assessing the kinetics of low affinity compounds.

David A Sykes, Palash Jain & Steven J Charlton

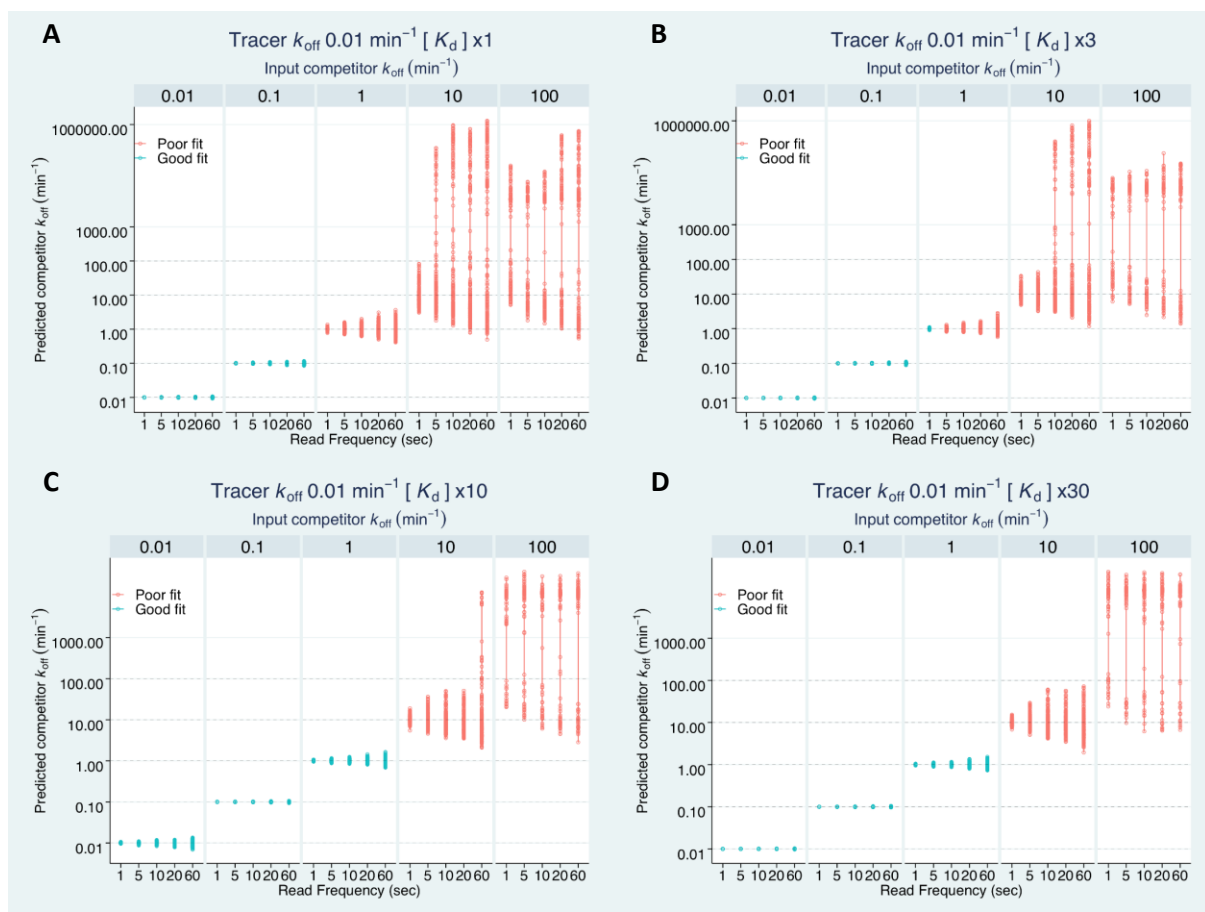


Supplemental Figure 1. Monte-Carlo simulation results exploring the effect of tracer kinetics and assay start and read frequency time on the accurate determination of competitor kinetic parameters representative of online addition protocol. Effect of assay read frequency on measured k_{off} of unlabelled competitor compounds with varied kinetics in competition with different concentrations of a slowly dissociating tracer with kinetic parameters; k_{off} of 10 min^{-1} , k_{on} of $3 \times 10^7 \text{ M}^{-1} \text{ min}^{-1}$. Tracer concentrations were (A) $1x K_d$, (B) $3x K_d$ (C) $10x K_d$ and (D) $30x K_d$. Blue open symbols represent conditions which returned $>90\%$ reliable fits. Red open symbols

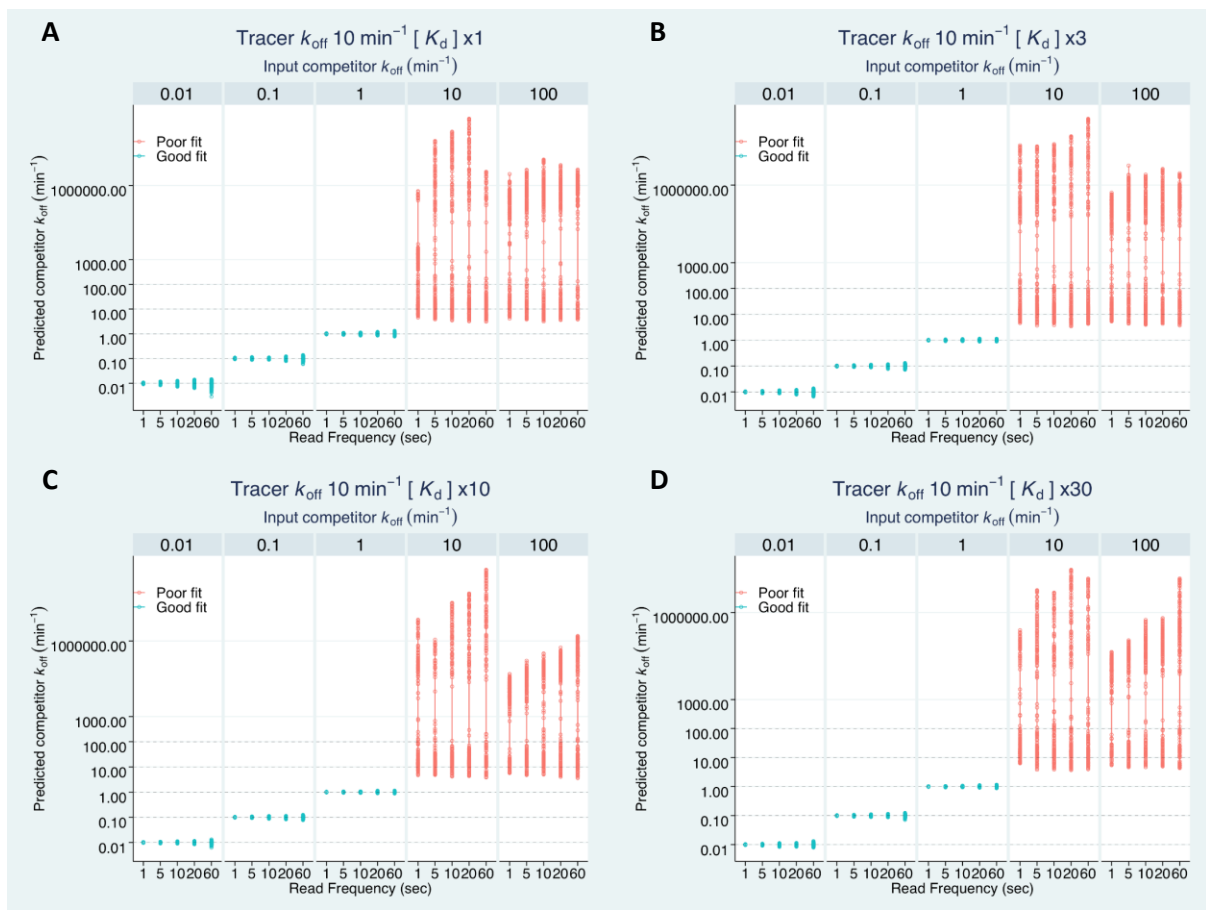
represent conditions which returned <90% reliable fits. In all cases tracer simulations were performed with an initial start time of 1sec representative of addition of receptor to a reaction containing free tracer (L) and unlabelled competitor (I), all of 200 values (minus outliers) for each simulated condition are plotted.



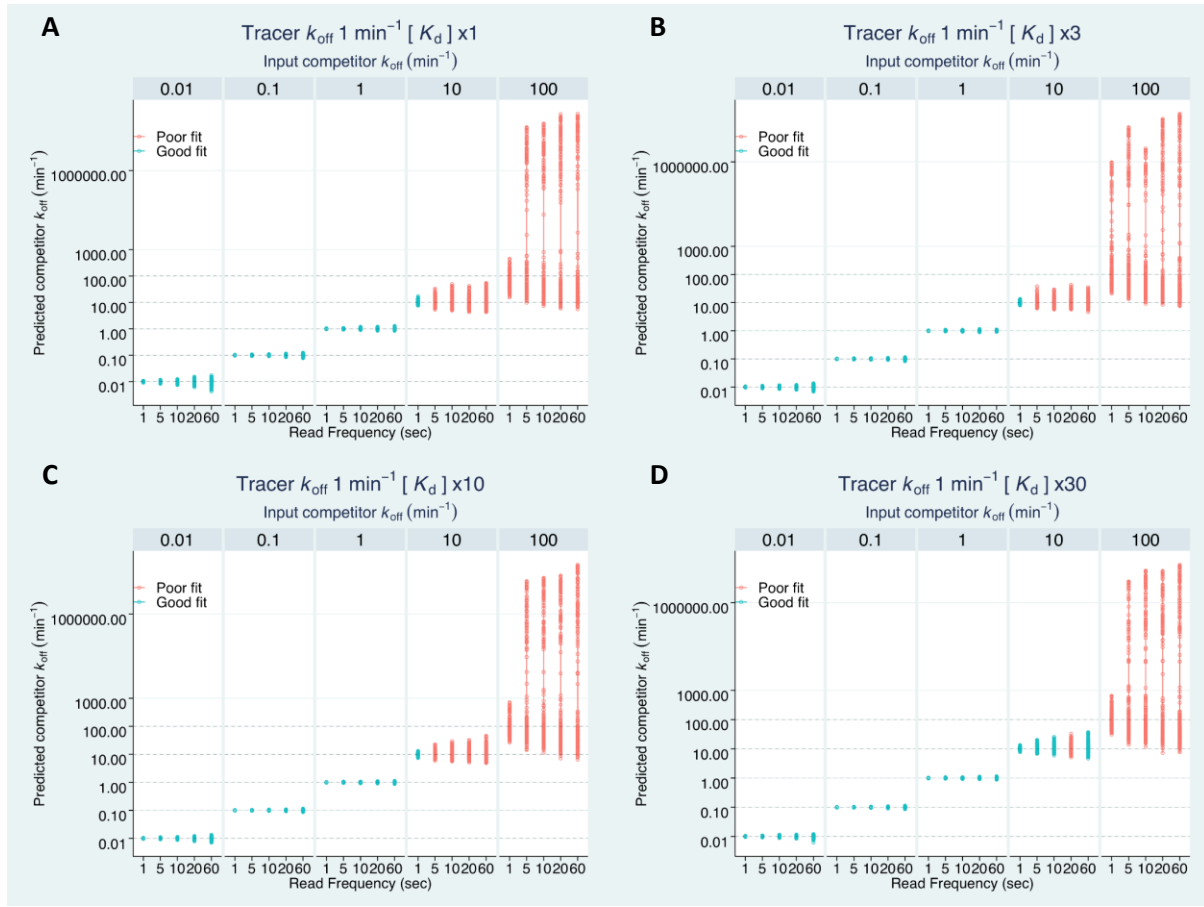
Supplemental Figure 2. Monte-Carlo simulation results exploring the effect of tracer kinetics and assay start and read frequency time on the accurate determination of competitor kinetic parameters representative of online addition protocol. Effect of assay read frequency on measured k_{off} of unlabelled competitor compounds with varied kinetics in competition with different concentrations of a slowly dissociating tracer with kinetic parameters; k_{off} of 1min^{-1} , k_{on} of $1 \times 10^7 \text{ M}^{-1} \text{ min}^{-1}$. Tracer concentrations were (A) $1x K_d$ (B) $3x K_d$ (C) $10x K_d$ and (D) $30x K_d$. Blue open symbols represent conditions which returned $>90\%$ reliable fits. Red open symbols represent conditions which returned $<90\%$ reliable fits. In all cases tracer simulations were performed with an initial start time of 1sec representative of addition of receptor to a reaction containing free tracer (L) and competitor (I), all of 200 values (minus outliers) for each simulated condition are plotted.



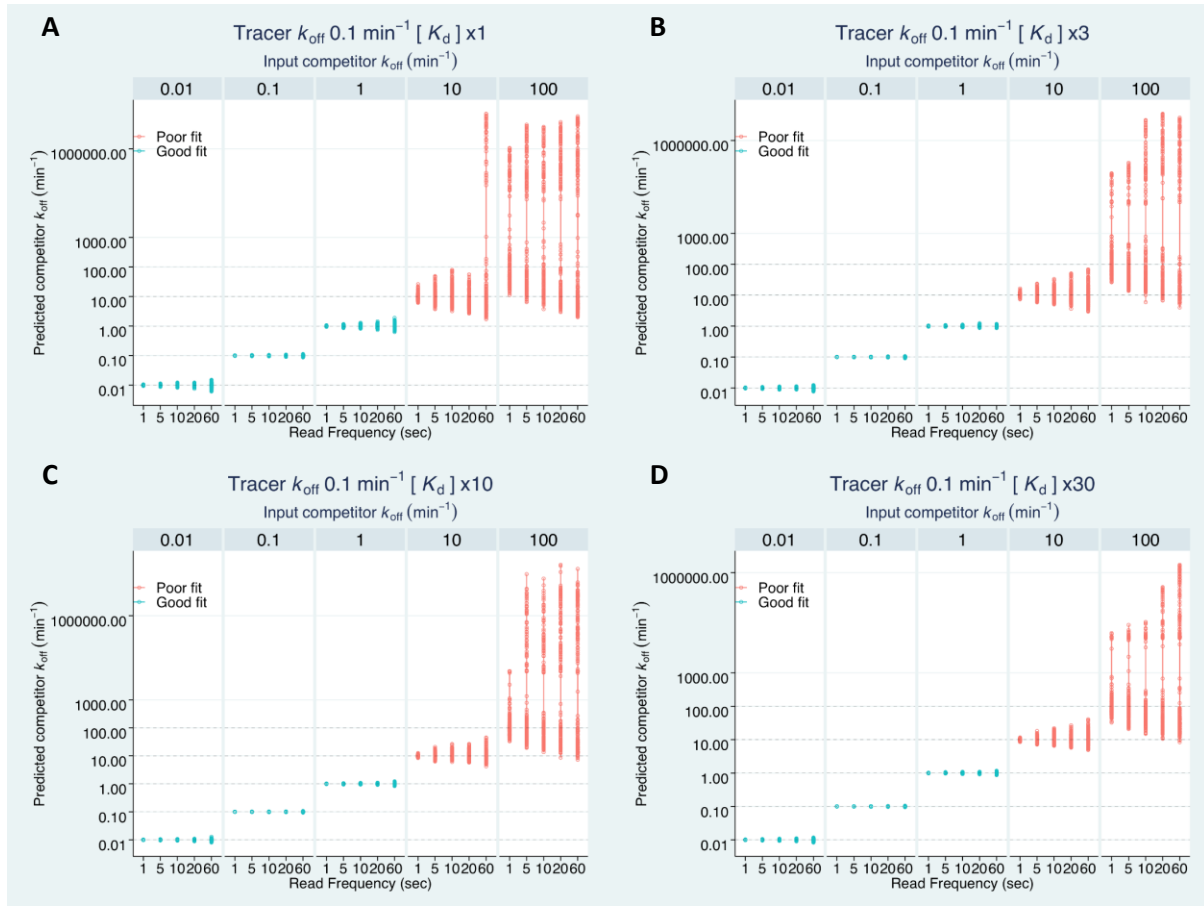
Supplemental Figure 3. Monte-Carlo simulation results exploring the effect of tracer kinetics and assay start and read frequency time on the accurate determination of competitor kinetic parameters representative of online addition protocol. Effect of assay read frequency on measured k_{off} of unlabelled competitor compounds with varied kinetics in competition with different concentrations of a slowly dissociating tracer with kinetic parameters; k_{off} of 0.01 min^{-1} , k_{on} of $1 \times 10^9 \text{ M}^{-1} \text{ min}^{-1}$. Tracer concentrations were **(A)** $1 \times K_d$ **(B)** $3 \times K_d$ **(C)** $10 \times K_d$ and **(D)** $30 \times K_d$. Blue open symbols represent conditions which returned $>90\%$ reliable fits. Red open symbols represent conditions which returned $<90\%$ reliable fits. In all cases tracer simulations were performed with an initial start time of 1 sec representative of addition of receptor to a reaction containing free tracer (L) and competitor (I), all of 200 values (minus outliers) for each simulated condition are plotted.



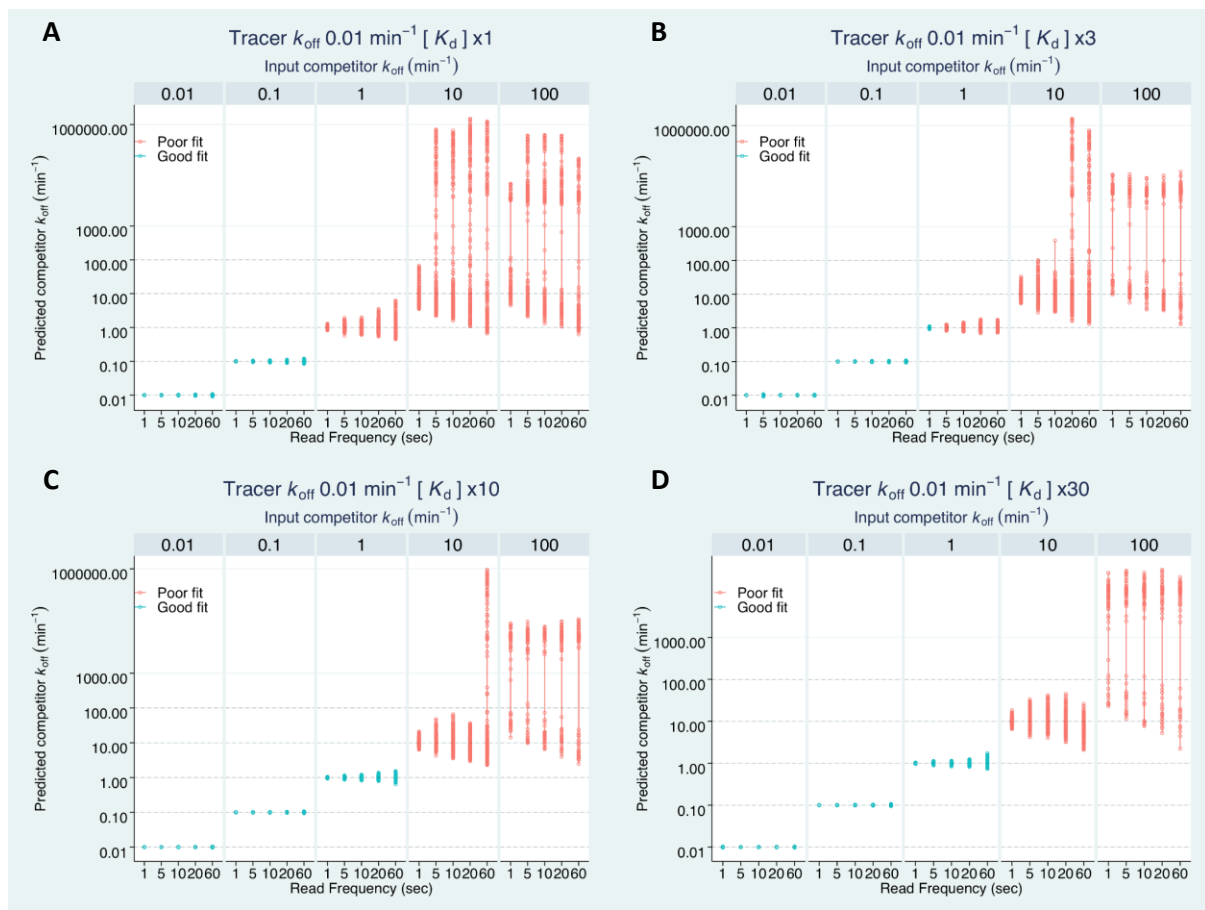
Supplemental Figure 4. Monte-Carlo simulation results exploring the effect of tracer kinetics and assay start and read frequency time on the accurate determination of competitor kinetic parameters representative of offline addition protocol. Effect of assay read frequency on measured k_{off} of unlabelled competitor compounds with varied kinetics in competition with different concentrations of a slowly dissociating tracer with kinetic parameters; k_{off} of 10min^{-1} , k_{on} of $3 \times 10^7 \text{ M}^{-1} \text{ min}^{-1}$. Tracer concentrations were (A) $1x K_d$ (B) $3x K_d$, (C) $10x K_d$ and (D) $30x K_d$. Blue open symbols represent conditions which returned $>90\%$ reliable fits. Red open symbols represent conditions which returned $<90\%$ reliable fits. In all cases tracer simulations were performed with an initial start time of 30sec representative of addition of receptor to a reaction containing free tracer (L) and competitor (I), all of 200 values (minus outliers) for each simulated condition are plotted.



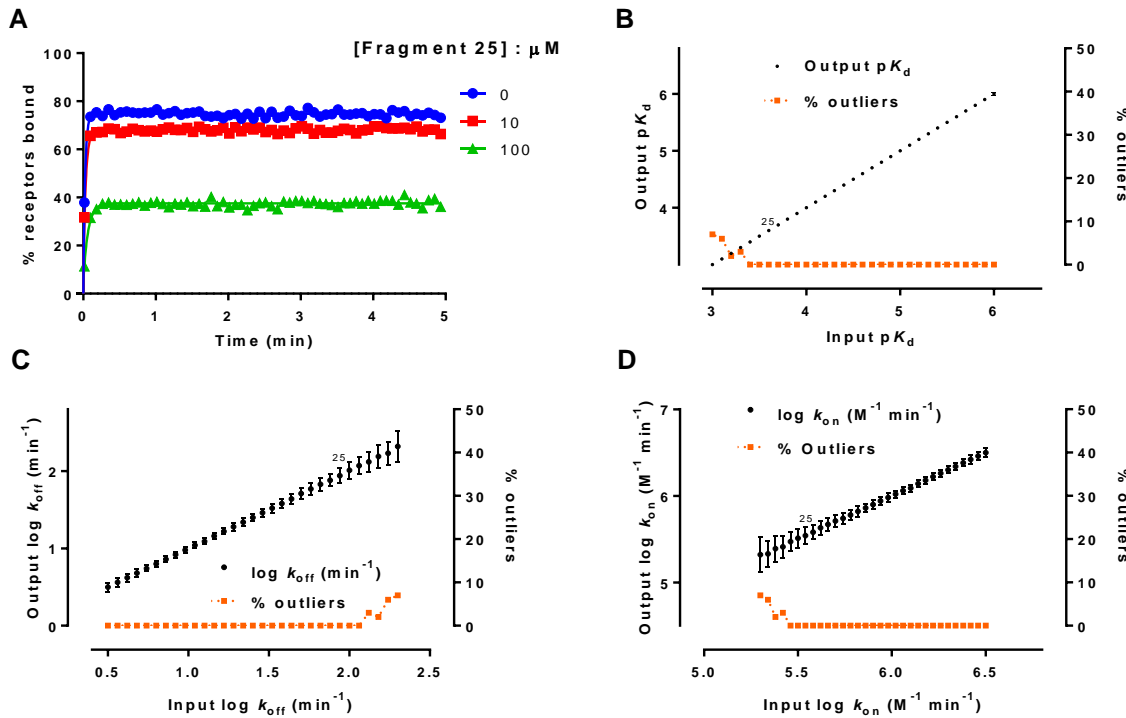
Supplemental Figure 5. Monte-Carlo simulation results exploring the effect of tracer kinetics and assay start and read frequency time on the accurate determination of competitor kinetic parameters representative of offline addition protocol. Effect of assay read frequency on measured k_{off} of unlabelled competitor compounds with varied kinetics in competition with different concentrations of a slowly dissociating tracer with kinetic parameters; k_{off} of 1 min^{-1} , k_{on} of $1 \times 10^7 \text{ min}^{-1}$. Tracer concentrations were **(A)** $1 \times K_d$ **(B)** $3 \times K_d$ **(C)** $10 \times K_d$ and **(D)** $30 \times K_d$. Blue open symbols represent conditions which returned $>90\%$ reliable fits. Red open symbols represent conditions which returned $<90\%$ reliable fits. In all cases tracer simulations were performed with an initial start time of 30sec representative of addition of receptor to a reaction containing free tracer (L) and competitor (I), all of 200 values (minus outliers) for each simulated condition are plotted.



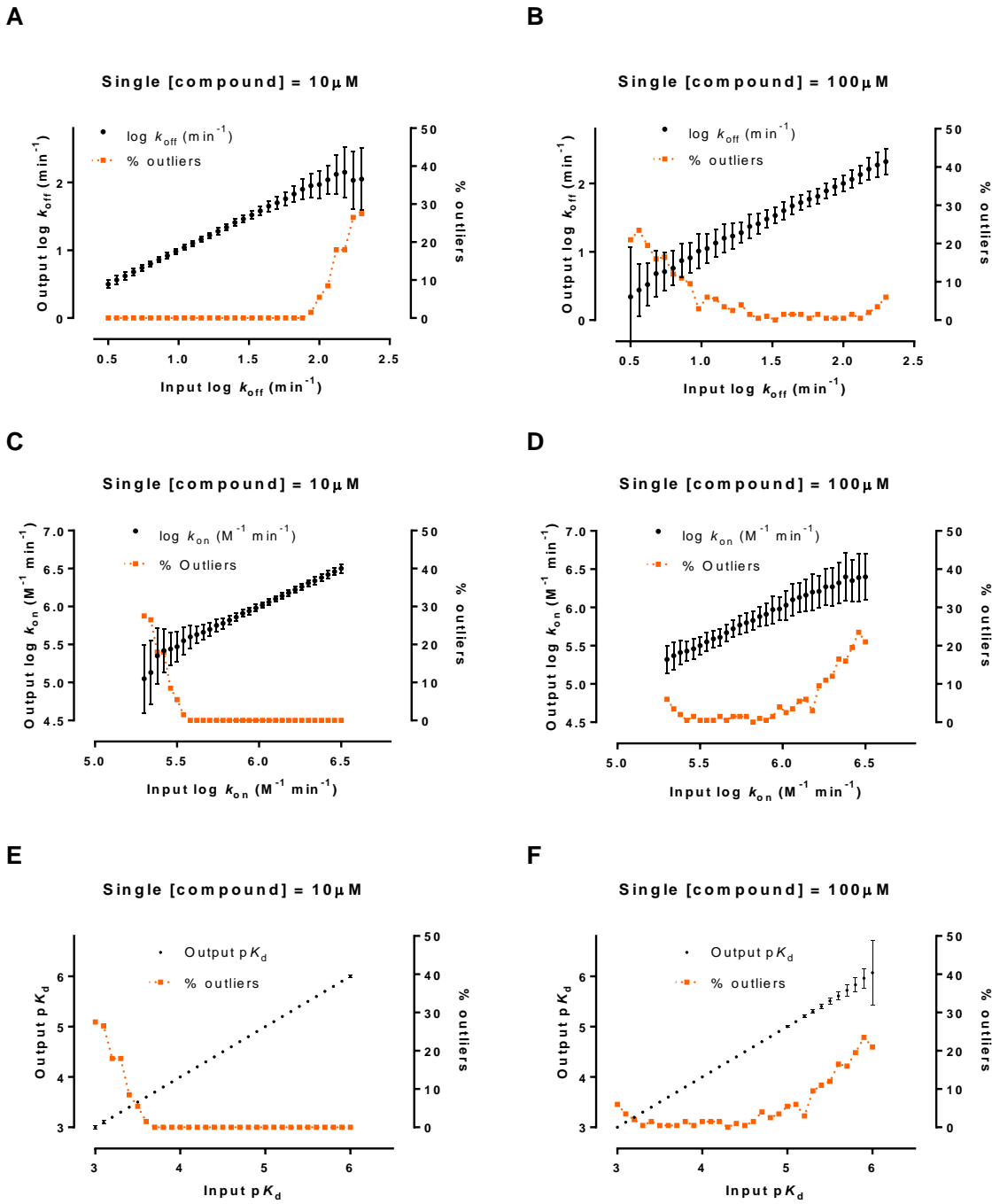
Supplemental Figure 6. Monte-Carlo simulation results exploring the effect of tracer kinetics and assay start and read frequency time on the accurate determination of competitor kinetic parameters representative of offline addition protocol. Effect of assay read frequency on measured k_{off} of unlabelled competitor compounds with varied kinetics in competition with different concentrations of a slowly dissociating tracer with kinetic parameters; k_{off} of 0.1 min⁻¹, k_{on} of 1×10^8 min⁻¹. Tracer concentrations were **(A)** 1x K_d , **(B)** 3x K_d , **(C)** 10x K_d and **(D)** 30x K_d . Blue open symbols represent conditions which returned >90% reliable fits. Red open symbols represent conditions which returned <90% reliable fits. In all cases tracer simulations were performed with an initial start time of 30sec representative of addition of receptor to a reaction containing free tracer (L) and competitor (I), all of 200 values (minus outliers) for each simulated condition are plotted.



Supplemental Figure 7. Monte-Carlo simulation results exploring the effect of tracer kinetics and assay start and read frequency time on the accurate determination of competitor kinetic parameters representative of offline addition protocol. Effect of assay read frequency on measured k_{off} of unlabelled competitor compounds with varied kinetics in competition with different concentrations of a slowly dissociating tracer with kinetic parameters; k_{off} of 0.01 min^{-1} , k_{on} of $1 \times 10^9 \text{ min}^{-1}$. Tracer concentrations were **(A)** $1 \times K_d$, **(B)** $3 \times K_d$, **(C)** $10 \times K_d$ and **(D)** $30 \times K_d$. Blue open symbols represent conditions which returned $>90\%$ reliable fits. Red open symbols represent conditions which returned $<90\%$ reliable fits. In all cases tracer simulations were performed with an initial start time of 30sec representative of addition of receptor to a reaction containing free tracer (L) and competitor (I), all of 200 values (minus outliers) for each simulated condition are plotted.



Supplemental Figure 8. Monte-Carlo simulation results representative of the competition profile observed between low affinity fragments 1 to 31 (affinities ranging from 1-1000 μM) tested at 10 and 100 μM in competition with a fixed concentration of a rapidly dissociating tracer. **(A)** Competition between a fixed concentration ($3 \times K_d$) of a rapidly dissociating tracer with the following kinetic parameters; k_{off} of 10 min^{-1} , k_{on} of $3 \times 10^7 \text{ M}^{-1} \text{ min}^{-1}$, and competitor fragment 25 with the following kinetic parameters; k_{off} of 87.1 min^{-1} , k_{on} of $5 \times 10^5 \text{ M}^{-1} \text{ min}^{-1}$, data shown are representative of 200 simulations. **(B)** Correlation between input K_d and output K_d , **(C)** between input k_{off} and output k_{off} , **(D)** between input k_{on} and output k_{on} . In each case tracer and competitor binding simulations were performed with an initial start time of 1sec (representative of injection of receptor to a reaction containing tracer) and a read frequency of 5sec, the data shown points shown in the correlations plots are the average of 200 simulations.



Supplemental Figure 9. Monte-Carlo simulation results representative of the competition profile observed between low affinity fragments (1-1000 μM) tested at 10 and 100 μM in competition with a fixed concentration (3x K_d) of a rapidly dissociating tracer with the following kinetic parameters; k_{off} of 10 min^{-1} , k_{on} of $3 \times 10^7 \text{ M}^{-1} \text{ min}^{-1}$. Correlation between **A)** input k_{off} and output k_{off} at 10 μM **B)** input k_{off} and output k_{off} at 100 μM . **C)** input k_{on} and output k_{off} at 10 μM . **D)** input k_{on} and output k_{off} at 100 μM . **E)** input K_d and output K_d , at 10 μM . **F)** input K_d and output K_d , at 100 μM . In each case tracer and competitor binding

simulations were performed with an initial start time of 1sec (representative of injection of receptor to a reaction containing tracer) and a read frequency of 5sec, the data shown points shown in the correlations plots are the average of 200 simulations.

Supplemental data files

Supplemental Table 1. Summary of the kinetic input parameters and their estimates for the tracer described in [Table 1](#), under conditions which mimic online and offline addition, determined from 200 simulated data sets using the global association model equation (see [Figure 1](#)).

Online injection first read time 1sec							
Number of : (Ambiguous fits; Outliers)	Read frequency (sec)	Input K_d (Output K_d) nM	K_d %CV	Input k_{on} (Output k_{on}) $M^{-1}min^{-1}$	k_{on} %CV	Input k_{off} (Output k_{off}) min^{-1}	k_{off} %CV
(0; 0)	1	333 (333)	0.21	3E7 (3E7)	1.29	10 (10.01)	1.32
(0; 0)	5	333 (333)	0.47	3E7 (3E7)	2.31	10 (10.01)	2.27
(0; 0)	10	333 (333)	0.72	3E7 (3E7)	2.49	10 (10.01)	2.50
(0; 0)	20	333 (334)	0.96	3E7 (3.01E7)	2.34	10 (10.05)	2.40
(0; 0)	60	333 (333)	1.67	3E7 (3E7)	2.72	10 (9.99)	3.07
<hr/>							
(0; 0)	1	100 (100)	0.26	1E7 (1E7)	0.44	1 (1.00)	0.53
(0; 0)	5	100 (100)	0.55	1E7 (1E7)	0.93	1 (1.00)	1.18
(0; 0)	10	100 (100)	0.81	1E7 (1E7)	1.34	1 (1.00)	1.71
(0; 0)	20	100 (100)	1.10	1E7 (1E7)	1.62	1 (1.00)	2.10
(0; 0)	60	100 (100)	2.14	1E7 (1E7)	2.74	1 (1.00)	3.52
<hr/>							
(0; 0)	1	1 (1)	0.14	1E8 (1E8)	0.14	0.1 (0.1)	0.22

(0; 0)	5	1 (1)	0.32	1E8 (1E8)	0.32	0.1 (0.1)	0.51
(0; 0)	10	1 (1)	0.49	1E8 (1E8)	0.40	0.1 (0.1)	0.70
(0; 0)	20	1 (1)	0.61	1E8 (1E8)	0.64	0.1 (0.1)	1.02
(0; 0)	60	1 (1)	1.03	1E8 (1E8)	1.14	0.1 (0.1)	1.75
 							
(0; 0)	1	0.01 (0.01)	0.29	1E9 (1E9)	0.06	0.01 (0.01)	0.32
(0; 0)	5	0.01 (0.01)	0.68	1E9 (1E9)	0.15	0.01 (0.01)	0.76
(0; 0)	10	0.01 (0.01)	0.91	1E9 (1E9)	0.20	0.01 (0.01)	1.02
(0; 0)	20	0.01 (0.01)	1.51	1E9 (1E9)	0.29	0.01 (0.01)	1.38
(0; 0)	60	0.01 (0.01)	2.50	1E9 (1E9)	0.55	0.01 (0.01)	2.19

Offline addition first read time 30 sec							
Number of : (Ambiguous fits; Outliers)	Read frequency (sec)	Input K_d (Output K_d) nM	K_d %CV	Input k_{on} (Output k_{on}) $M^{-1}min^{-1}$	k_{on} %CV	Input k_{off} (Output k_{off}) min^{-1}	k_{off} %CV
(197; 0)	1	333 (333)	0.21	3E7 (1.12E7)	41.38	10 (37.17)	41.36
(199; 8)	5	333 (333)	0.44	3E7 (1.71E8)	4.92	10 (56.90)	4.86
(200; 2)	10	333 (333)	0.72	3E7 (2.30E8)	9.54	10 (76.78)	9.54
(192; 0)	20	333 (333)	0.95	3E7 (1.67E8)	31.98	10 (55.54)	32.02
(139; 2)	60	333 (333)	1.68	3E7 (1.13E8)	92.76	10 (37.69)	92.28

(0; 0)	1	100 (100)	0.27	1E7 (9.66E6)	0.67	1 (1.00)	0.80
(0; 0)	5	100 (100)	0.55	1E7 (1E7)	1.47	1 (1.00)	1.74
(0; 0)	10	100 (100)	0.83	1E7 (1E7)	2.08	1 (1.00)	2.50
(0; 0)	20	100 (100)	1.16	1E7 (1E7)	2.65	1 (1.00)	3.09
(0; 0)	60	100 (100)	1.94	1E7 (1E7)	3.39	1 (1.00)	4.27
<hr/>							
(0; 0)	1	1 (1)	0.14	1E8 (1E8)	0.13	0.1 (0.1)	0.22
(0; 0)	5	1 (1)	0.33	1E8 (1E8)	0.33	0.1 (0.1)	0.52
(0; 0)	10	1 (1)	0.44	1E8 (1E8)	0.47	0.1 (0.1)	0.72
(0; 0)	20	1 (1)	0.63	1E8 (1E8)	0.63	0.1 (0.1)	0.97
(0; 0)	60	1 (1)	1.03	1E8 (1E8)	1.17	0.1 (0.1)	1.77
<hr/>							
(0; 0)	1	0.01 (0.01)	0.30	1E9 (1E9)	0.06	0.01 (0.01)	0.33
(0; 0)	5	0.01 (0.01)	0.68	1E9 (1E9)	0.15	0.01 (0.01)	0.77
(0; 0)	10	0.01 (0.099)	0.94	1E9 (1E9)	0.20	0.01 (0.01)	1.05
(0; 0)	20	0.01 (0.01)	1.25	1E9 (1E9)	0.31	0.01 (0.01)	1.41
(0; 0)	60	0.01 (0.01)	2.30	1E9 (9.99E8)	0.53	0.01 (0.01)	2.61

Supplemental Table 2. Summary of the kinetic input parameters and their estimates for unlabelled compounds under conditions which mimic online injection and offline addition of membranes, values are determined from 200 simulated data sets using the Motulsky-Mahan model equation and the very low affinity tracer ($k_{\text{on}} = 3 \times 10^7 \text{ M}^{-1}\text{min}^{-1}$; $k_{\text{off}} = 10 \text{ min}^{-1}$ $K_d = 3 \mu\text{M}$).

Online injection first read time 1sec							
Number of : (Ambiguous fits; Outliers)	Read frequency (sec)	Input K_d (Output K_d)	K_d %CV	Input k_{on} (Output k_{on}) $\text{M}^{-1}\text{min}^{-1}$	k_{on} %CV	Input k_{off} (Output k_{off}) min^{-1}	k_{off} %CV
(0; 0)	1	10pM (10pM)	1.62	1E9 (1E9)	0.18	0.01 (0.01)	1.77
(0; 0)	5	10pM (10pM)	3.44	1E9 (1E9)	0.41	0.01 (0.01)	3.78
(0; 0)	10	10pM (10pM)	5.29	1E9 (1E9)	0.57	0.01 (0.01)	5.74
(0; 0)	20	10pM (10pM)	6.82	1E9 (1E9)	0.78	0.01 (0.01)	7.42
(0; 0)	60	10pM (10pM)	12.75	1E9 (0.999E8)	1.32	0.01 (0.01)	13.70
<hr/>							
(0; 0)	1	1nM (1nM)	1.12	1E8 (1E8)	0.34	0.1 (0.1)	1.38
(0; 0)	5	1nM (0.99nM)	2.73	1E8 (1E8)	0.78	0.1 (0.1)	3.29
(0; 0)	10	1nM (1nM)	3.98	1E8 (1E8)	1.29	0.1 (0.1)	4.99
(0; 0)	20	1nM (0.996nM)	5.37	1E8 (1E8)	1.51	0.1 (0.1)	6.49
(0; 0)	60	1nM (0.991nM)	12.13	1E8 (1E8)	3.31	0.1 (0.1)	14.79
<hr/>							
(0; 0)	1	100nM (100nM)	0.30	1E7 (9.99E6)	0.68	1 (1)	0.77
(0; 0)	5	100nM (99.9nM)	0.62	1E7 (1E7)	1.47	1 (1)	1.64

(0; 0)	10	100nM (100nM)	0.90	1E7 (1E7)	2.06	1 (1)	2.38
(0; 0)	20	100nM (99.9nM)	1.42	1E7 (1E7)	2.94	1 (1)	3.42
(0; 0)	60	100nM (99.8nM)	2.47	1E7 (1.01E7)	6.86	1 (1.01)	7.42
(0; 0)	1	10μM (10μM)	0.25	1E6 (1E6)	2.06	10 (10)	2.08
(0; 0)	5	10μM (10μM)	0.62	1E6 (1E6)	5.68	10 (10.02)	5.74
(0; 0)	10	10μM (10μM)	0.92	1E6 (1.01E6)	7.27	10 (10.05)	7.33
(0; 0)	20	10μM (9.99μM)	1.30	1E6 (1.01E6)	6.94	10 (10.05)	7.03
(0; 0)	60	10μM (9.98μM)	2.54	1E6 (1.01E6)	7.93	10 (10.06)	7.73
(0; 0)	1	1mM (1mM)	0.26	1E5 (9.98E4)	14.41	100 (99.81)	14.42
(0; 0)	5	1mM (1mM)	0.58	1E5 (1.04E5)	20.54	100 (103.86)	20.57
(0; 0)	10	1mM (1mM)	0.86	1E5 (1.03E5)	18.60	100 (103.48)	18.71
(0; 0)	20	1mM (1mM)	1.14	1E5 (1.02E5)	16.86	100 (101.83)	17.11
(0; 1)	60	1mM (1mM)	2.36	1E5 (1.02E5)	17.26	100 (102.38)	17.57

Offline addition first read time 30 sec							
Number of : (Ambiguous fits; Outliers)	Read frequency (sec)	Input K_d (Output K_d)	K_d %CV	Input k_{on} (Output k_{on}) $M^{-1}min^{-1}$	k_{on} %CV	Input k_{off} (Output k_{off}) min^{-1}	k_{off} %CV

(0; 0)	1	10pM (10pM)	1.55	1E9 (1E9)	0.17	0.01 (0.01)	1.67
(0; 0)	5	10pM (9.98pM)	3.74	1E9 (1E9)	0.43	0.01 (0.01)	4.09
(0; 0)	10	10pM (10pM)	4.95	1E9 (1E9)	0.56	0.01 (0.01)	5.43
(0; 0)	20	10pM (10pM)	6.79	1E9 (1E9)	0.86	0.01 (0.01)	7.47
(0; 0)	60	10pM (9.94pM)	12.31	1E9 (1E9)	1.42	0.01 (0.01)	13.39
(0; 0)	1	1nM (0.999nM)	1.24	1E8 (1E8)	0.37	0.1 (0.1)	1.52
(0; 0)	5	1nM (1nM)	2.68	1E8 (1E8)	0.90	0.1 (0.1)	3.39
(0; 0)	10	1nM (1nM)	3.79	1E8 (1E8)	1.24	0.1 (0.1)	4.77
(0; 0)	20	1nM (1nM)	5.42	1E8 (1E8)	1.70	0.1 (0.1)	6.73
(0; 0)	60	1nM (0.998nM)	9.62	1E8 (1E8)	2.78	0.1 (0.1)	11.83
(0; 0)	1	100nM (100nM)	0.33	1E7 (1E7)	1.04	1 (1)	1.18
(0; 0)	5	100nM (100nM)	0.70	1E7 (1E7)	2.18	1 (1)	2.38
(0; 0)	10	100nM (100nM)	0.92	1E7 (1E7)	3.05	1 (1)	3.30
(0; 0)	20	100nM (100nM)	1.41	1E7 (9.99E6)	4.28	1 (1)	4.79
(0; 0)	60	100nM (100nM)	1.30	1E7 (1E7)	3.85	1 (1)	4.26
(193; 6)	1	10μM (10μM)	0.28	1E6 (2.42E11)	277.73	10 (2.42E6)	277.65
(192; 19)	5	10μM (10μM)	0.58	1E6 (2.43E11)	261.24	10 (2.44E6)	261.33

(187; 27)	10	10µM (10µM)	0.93	1E6 (3.21E11)	241.99	10 (3.20E6)	241.45
(174; 30)	20	10µM (9.98µM)	1.18	1E6 (5.96E11)	258.44	10 (5.96E6)	258.67
(177; 31)	60	10µM (10µM)	2.19	1E6 (2.70E12)	275.64	10 (2.70E7)	275.21
(197; 0)	1	1mM (1mM)	0.26	1E5 (7.89E7)	143.79	100 (78893.74)	143.79
(191; 5)	5	1mM (1mM)	0.62	1E5 (3.01E8)	209.63	100 (3.01E5)	209.59
(188; 9)	10	1mM (1mM)	0.87	1E5 (2.50E8)	205.46	100 (2.51E5)	205.66
(192; 22)	20	1mM (9.99E-4)	1.14	1E5 (3.84E8)	209.43	100 (3.84E5)	209.53
(191; 36)	60	1mM (1mM)	1.51	1E5 (3.29E8)	170.69	100 (3.30E5)	171.09

Supplemental Table 3. Summary of the kinetic input parameters and their estimates for unlabelled compounds under conditions which mimic online injection and offline addition of membranes, values are determined from 200 simulated data sets using the Motulsky-Mahan model equation and the low affinity tracer ($k_{\text{on}} = 1 \times 10^7 \text{ M}^{-1} \text{ min}^{-1}$; $k_{\text{off}} = 1 \text{ min}^{-1}$ $K_d = 0.1 \mu\text{M}$).

Online injection first read time 1sec							
Number of : (Ambiguous fits; Outliers)	Read frequency (sec)	Input K_d (Output K_d)	K_d %CV	Input k_{on} (Output k_{on}) $\text{M}^{-1} \text{ min}^{-1}$	k_{on} %CV	Input k_{off} (Output k_{off}) min^{-1}	k_{off} %CV
(0; 0)	1	10pM (10.03pM)	1.72	1E9 (1E9)	0.21	0.01 (0.01)	1.90
(0; 0)	5	10pM (10.01pM)	3.49	1E9 (1E9)	0.38	0.01 (0.01)	3.78
(0; 0)	10	10pM (10.03pM)	5.17	1E9 (1E9)	0.61	0.01 (0.01)	5.68
(0; 0)	20	10pM (9.96pM)	8.02	1E9 (1E9)	0.90	0.01 (0.01)	8.75
(0; 0)	60	10pM (9.97pM)	12.56	1E9 (0.999E8)	1.49	0.01 (0.01)	13.80
<hr/>							
(0; 0)	1	1nM (1nM)	0.48	1E8 (1E8)	0.32	0.1 (0.1)	0.74
(0; 0)	5	1nM (0.9993nM)	1.05	1E8 (1E8)	0.66	0.1 (0.1)	1.53
(0; 0)	10	1nM (1nM)	1.54	1E8 (1E8)	0.98	0.1 (0.1)	2.32
(0; 0)	20	1nM (0.996nM)	2.25	1E8 (9.99E7)	1.35	0.1 (0.1)	3.22
(0; 0)	60	1nM (1.002nM)	4.06	1E8 (1E8)	2.67	0.1 (0.1)	6.12
<hr/>							
(0; 0)	1	100nM (100nM)	0.20	1E7 (1E7)	0.81	1 (1)	0.88
(0; 0)	5	100nM (100nM)	0.47	1E7 (9.99E6)	1.41	1 (1)	1.53

(0; 0)	10	100nM (100nM)	0.62	1E7 (1E7)	2.20	1 (1)	2.29
(0; 0)	20	100nM (100nM)	0.90	1E7 (1E7)	3.24	1 (1)	3.48
(0; 0)	60	100nM (100nM)	1.67	1E7 (1E7)	7.85	1 (1)	8.46
<hr/>							
(0; 0)	1	10μM (10μM)	0.18	1E6 (1.01E6)	4.04	10 (10.07)	4.07
(0; 0)	5	10μM (10μM)	0.43	1E6 (1.01E6)	9.08	10 (10.06)	9.13
(0; 0)	10	10μM (10μM)	0.64	1E6 (1.01E6)	13.24	10 (10.14)	13.32
(0; 0)	20	10μM (10μM)	0.85	1E6 (1.06E6)	27.32	10 (10.57)	27.51
(0; 4)	60	10μM (10μM)	1.52	1E6 (1.03E6)	48.92	10 (10.29)	49.03
<hr/>							
(200; 4)	1	1mM (1mM)	0.19	1E5 (1.07E5)	35.44	100 (107.40)	35.47
(194; 23)	5	1mM (1mM)	0.47	1E5 (1.45E5)	96.89	100 (145.64)	97.11
(188; 30)	10	1mM (1mM)	0.56	1E5 (1.25E5)	82.92	100 (124.57)	82.98
(161; 34)	20	1mM (1mM)	0.89	1E5 (1.10E5)	84.50	100 (109.54)	84.29
(110; 54)	60	1mM (1mM)	1.51	1E5 (1.08E5)	79.17	100 (108.44)	79.07

Offline addition first read time 30 sec							
Number of : (Ambiguous fits; Outliers)	Read frequency (sec)	Input K_d (Output K_d)	K_d %CV	Input k_{on} (Output k_{on}) $M^{-1}min^{-1}$	k_{on} %CV	Input k_{off} (Output k_{off}) min^{-1}	k_{off} %CV

(0; 0)	1	10pM (10.02pM)	1.59	1E9 (1E9)	0.19	0.01 (0.01)	1.74
(0; 0)	5	10pM (10.02pM)	3.85	1E9 (1E9)	0.43	0.01 (0.01)	4.20
(0; 0)	10	10pM (10.02pM)	5.34	1E9 (1E9)	0.63	0.01 (0.01)	5.85
(0; 0)	20	10pM (10.05pM)	7.15	1E9 (1E9)	0.81	0.01 (0.01)	7.77
(0; 0)	60	10pM (9.73pM)	13.56	1E9 (9.97E8)	1.53	0.01 (0.01)	14.84
(0; 0)	1	1nM (1nM)	0.53	1E8 (1E8)	0.33	0.1 (0.1)	0.77
(0; 0)	5	1nM (1nM)	1.10	1E8 (9.99E7)	0.79	0.1 (0.1)	1.70
(0; 0)	10	1nM (1nM)	1.52	1E8 (1E8)	1.01	0.1 (0.1)	2.30
(0; 0)	20	1nM (1.002nM)	2.36	1E8 (1E8)	1.44	0.1 (0.1)	3.37
(0; 0)	60	1nM (1.002nM)	3.59	1E8 (1E8)	2.45	0.1 (0.1)	5.39
(0; 0)	1	100nM (100nM)	0.22	1E7 (1E7)	0.87	1 (1)	0.96
(0; 0)	5	100nM (100nM)	0.44	1E7 (1E7)	2.07	1 (1)	2.15
(0; 0)	10	100nM (100nM)	0.67	1E7 (1E7)	2.67	1 (1)	2.85
(0; 0)	20	100nM (99.99nM)	0.91	1E7 (1E7)	3.92	1 (1)	4.14
(0; 0)	60	100nM (100nM)	0.97	1E7 (1E7)	3.75	1 (1)	3.96
(10; 0)	1	10μM (9.998μM)	0.21	1E6 (1.02E6)	11.41	10 (10.22)	11.46
(25; 0)	5	10μM (9.998μM)	0.41	1E6 (1.06E6)	35.34	10 (10.60)	35.44

(24; 9)	10	10µM (9.998µM)	0.64	1E6 (1.01E6)	36.20	10 (11.02)	36.30
(33; 5)	20	10µM (10µM)	0.95	1E6 (1.21E6)	53.14	10 (12.14)	53.50
(15; 11)	60	10µM (10µM)	1.50	1E6 (1.13E6)	48.06	10 (11.35)	48.33
(200; 23)	1	1mM (0.994mM)	0.19	1E5 (6.05E7)	312.35	100 (6.06E4)	312.28
(200; 12)	5	1mM (1mM)	0.44	1E5 (1.47E9)	249.83	100 (1.47E6)	249.81
(192; 33)	10	1mM (1mM)	0.65	1E5 (2.15E8)	273.44	100 (2.16E5)	273.47
(173; 13)	20	1mM (9.99E-4)	0.91	1E5 (2.83E9)	236.28	100 (2.83E6)	235.84
(138; 11)	60	1mM (9.98E-4)	1.42	1E5 (4.33E9)	252.26	100 (4.34E6)	252.33

Supplemental Table 4. Summary of the kinetic input parameters and their estimates for unlabelled compounds under conditions which mimic online injection and offline addition of membranes, values are determined from 200 simulated data sets using the Motulsky-Mahan model equation and the low affinity tracer ($k_{\text{on}} = 1 \times 10^8 \text{ M}^{-1} \text{ min}^{-1}$; $k_{\text{off}} = 0.1 \text{ min}^{-1}$ $K_d = 1 \text{ nM}$).

Online injection first read time 1sec							
Number of : (Ambiguous fits; Outliers)	Read frequency (sec)	Input K_d (Output K_d)	K_d %CV	Input k_{on} (Output k_{on}) $\text{M}^{-1} \text{ min}^{-1}$	k_{on} %CV	Input k_{off} (Output k_{off}) min^{-1}	k_{off} %CV
(0; 0)	1	10pM (10pM)	1.07	1E9 (1E9)	0.18	0.01 (0.01)	1.22
(0; 0)	5	10pM (9.99pM)	2.41	1E9 (1E9)	0.42	0.01 (0.01)	2.74
(0; 0)	10	10pM (10pM)	3.52	1E9 (1E9)	0.62	0.01 (0.01)	4.06
(0; 0)	20	10pM (10pM)	5.05	1E9 (1E9)	0.88	0.01 (0.01)	5.05
(0; 0)	60	10pM (10pM)	8.33	1E9 (1E9)	1.54	0.01 (0.01)	9.55
<hr/>							
(0; 0)	1	1nM (1nM)	0.17	1E8 (1E8)	0.29	0.1 (0.1)	0.38
(0; 0)	5	1nM (0.9993nM)	0.38	1E8 (1E8)	0.57	0.1 (0.1)	0.75
(0; 0)	10	1nM (1nM)	0.56	1E8 (1E8)	0.92	0.1 (0.1)	1.24
(0; 0)	20	1nM (0.999nM)	0.81	1E8 (9.98E7)	1.27	0.1 (0.1)	1.73
(0; 0)	60	1nM (0.999nM)	1.34	1E8 (9.99E7)	2.04	0.1 (0.1)	2.78
<hr/>							
(0; 0)	1	100nM (100nM)	0.12	1E7 (1E7)	1.23	1 (1)	1.27
(0; 0)	5	100nM (100nM)	0.25	1E7 (1.01E7)	3.10	1 (1)	3.20

(0; 0)	10	100nM (100nM)	0.38	1.01E7 (1E7)	4.0	1 (1.01)	4.15
(0; 0)	20	100nM (100nM)	0.59	1E7 (9.99E6)	6.0	1 (1)	6.17
(0; 0)	60	100nM (99.9nM)	0.99	1E7 (1.02E7)	10.71	1 (1.02)	10.87
(198; 0)	1	10μM (10μM)	0.12	1E6 (1.01E6)	11.55	10 (10.07)	11.57
(167; 1)	5	10μM (10μM)	0.27	1E6 (1.08E6)	30.83	10 (10.84)	30.90
(165; 6)	10	10μM (10μM)	0.35	1E6 (1.17E6)	46.26	10 (11.74)	46.37
(145; 12)	20	10μM (10μM)	0.51	1E6 (1.14E6)	52.10	10 (11.45)	52.30
(138; 38)	60	10μM (9.99μM)	0.98	1E6 (1.31E6)	104.83	10 (13.12)	104.98
(200; 29)	1	1mM (1mM)	0.12	1E5 (3.79E6)	283.24	100 (3789.78)	283.25
(200; 6)	5	1mM (1mM)	0.27	1E5 (1.72E8)	251.19	100 (1.72E5)	251.26
(200; 35)	10	1mM (0.994mM)	7.82	1E5 (2.89E7)	261.12	100 (2.56E4)	245.84
(197; 24)	20	1mM (1mM)	0.54	1E5 (2.52E8)	277.58	100 (2.52E5)	277.30
(175; 13)	60	1mM (1mM)	0.86	1E5 (1.18E9)	240.35	100 (1.18E6)	240.04

Offline addition first read time 30 sec							
Number of : (Ambiguous fits; Outliers)	Read frequency (sec)	Input K_d (Output K_d)	K_d %CV	Input k_{on} (Output k_{on}) $M^{-1}min^{-1}$	k_{on} %CV	Input k_{off} (Output k_{off}) min^{-1}	k_{off} %CV

(0; 0)	1	10pM (10.02pM)	1.21	1E9 (1E9)	0.20	0.01 (0.01)	1.38
(0; 0)	5	10pM (9.99pM)	2.37	1E9 (1E9)	0.43	0.01 (0.01)	2.73
(0; 0)	10	10pM (10.02pM)	3.72	1E9 (1E9)	0.59	0.01 (0.01)	4.21
(0; 0)	20	10pM (10.1pM)	4.55	1E9 (1E9)	0.86	0.01 (0.01)	5.23
(0; 0)	60	10pM (10pM)	8.39	1E9 (9.97E8)	1.51	0.01 (0.01)	9.60
(0; 0)	1	1nM (1nM)	0.17	1E8 (1E8)	0.27	0.1 (0.1)	0.38
(0; 0)	5	1nM (1nM)	0.37	1E8 (1E8)	0.66	0.1 (0.1)	0.88
(0; 0)	10	1nM (1nM)	0.50	1E8 (1E8)	0.88	0.1 (0.1)	1.14
(0; 0)	20	1nM (1nM)	0.74	1E8 (1E8)	1.35	0.1 (0.1)	1.78
(0; 0)	60	1nM (1nM)	1.27	1E8 (1E8)	2.34	0.1 (0.1)	3.13
(0; 0)	1	100nM (100nM)	0.28	1E7 (1E7)	1.57	1 (1)	1.71
(0; 0)	5	100nM (100nM)	0.44	1E7 (1E7)	2.07	1 (1)	2.15
(0; 0)	10	100nM (100nM)	0.35	1E7 (9.96E6)	3.76	1 (1)	3.80
(0; 0)	20	100nM (100nM)	0.51	1E7 (1E7)	5.80	1 (1)	5.91
(0; 0)	60	100nM (100nM)	0.55	1E7 (1E7)	5.52	1 (1)	5.64
(200; 0)	1	10μM (10μM)	0.11	1E6 (1.05E6)	13.71	10 (10.47)	13.74
(189; 5)	5	10μM (10μM)	0.26	1E6 (1.10E6)	30.09	10 (10.96)	30.17

(160; 3)	10	10µM (10µM)	0.35	1E6 (1.11E6)	44.94	10 (11.10)	45.04
(146; 9)	20	10µM (10µM)	0.51	1E6 (1.21E6)	67.30	10 (12.15)	67.49
(127; 32)	60	10µM (9.98µM)	0.96	1E6 (1.33E6)	90.67	10 (13.30)	91.04
(200; 16)	1	1mM (0.994mM)	7.39	1E5 (5.92E6)	326.01	100 (5.30E3)	328.85
(200; 36)	5	1mM (1mM)	0.25	1E5 (1.51E7)	248.87	100 (1.51E4)	249.0
(199; 8)	10	1mM (1mM)	0.33	1E5 (3.17E8)	283.26	100 (3.17E5)	283.26
(173; 23)	20	1mM (9.99E-4)	0.96	1E5 (6.49E8)	235.89	100 (2.83E6)	235.57
(180; 13)	60	1mM (1mM)	0.99	1E5 (5.02E8)	217.62	100 (5.02E5)	217.31

Supplemental Table 5. Summary of the kinetic input parameters and their estimates for unlabelled compounds under conditions which mimic online injection and offline addition of membranes, values are determined from 200 simulated data sets using the Motulsky-Mahan model equation and the low affinity tracer ($k_{\text{on}} = 1 \times 10^9 \text{ M}^{-1} \text{ min}^{-1}$; $k_{\text{off}} = 0.01 \text{ min}^{-1}$ $K_d = 10 \text{ pM}$).

Online injection first read time 1sec							
Number of : (Ambiguous fits; Outliers)	Read frequency (sec)	Input K_d (Output K_d)	K_d %CV	Input k_{on} (Output k_{on}) $\text{M}^{-1} \text{ min}^{-1}$	k_{on} %CV	Input k_{off} (Output k_{off}) min^{-1}	k_{off} %CV
(0; 0)	1	10pM (10pM)	0.10	1E9 (1E9)	0.11	0.01 (0.01)	0.18
(0; 0)	5	10pM (10pM)	0.22	1E9 (1E9)	0.25	0.01 (0.01)	0.41
(0; 0)	10	10pM (10pM)	0.33	1E9 (1E9)	0.34	0.01 (0.01)	0.61
(0; 0)	20	10pM (10pM)	0.45	1E9 (1E9)	0.54	0.01 (0.01)	0.89
(0; 0)	60	10pM (10pM)	0.86	1E9 (9.99E8)	0.84	0.01 (0.01)	1.51
<hr/>							
(0; 0)	1	1nM (1nM)	0.05	1E8 (1E8)	0.44	0.1 (0.1)	0.46
(0; 0)	5	1nM (1nM)	0.12	1E8 (1E8)	0.88	0.1 (0.1)	0.93
(0; 0)	10	1nM (1nM)	0.17	1E8 (1E8)	1.47	0.1 (0.1)	1.51
(0; 0)	20	1nM (1nM)	0.24	1E8 (1E8)	1.92	0.1 (0.1)	2.01
(0; 0)	60	1nM (1nM)	0.47	1E8 (1E8)	3.53	0.1 (0.1)	3.75
<hr/>							
(7; 0)	1	100nM (100nM)	0.05	1E7 (9.97E6)	3.58	1 (1)	3.59
(43; 0)	5	100nM (100nM)	0.11	1E7 (1.01E7)	8.31	1 (1.01)	8.36

(50; 0)	10	100nM (100nM)	0.15	1E7 (1.01E7)	11.68	1 (1.01)	11.74
(66; 0)	20	100nM (100nM)	0.22	1E7 (1.03E7)	15.59	1 (1.03)	15.65
(80; 2)	60	100nM (99.9nM)	0.37	1E7 (1.07E7)	35.12	1 (1.07)	35.29
1							
(200; 1)	1	10μM (10μM)	0.05	1E6 (1.15E6)	43.79	10 (11.52)	43.81
(200; 29)	5	10μM (10μM)	0.12	1E6 (1.12E6)	66.90	10 (11.25)	66.95
(200; 14)	10	10μM (10μM)	0.16	1E6 (1.75E9)	294.79	10 (17548.04)	294.76
(200; 8)	20	10μM (10μM)	0.24	1E6 (5.64E9)	250.94	10 (56466.86)	251.01
(200; 6)	60	10μM (10μM)	0.39	1E6 (8.72E9)	230.45	10 (87216.14)	230.35
2							
(200; 11)	1	1mM (1mM)	0.05	1E5 (9.55E6)	48.48	100 (9553.29)	48.47
(200; 21)	5	1mM (1mM)	0.12	1E5 (9.79E6)	54.05	100 (9787.06)	54.05
(200; 16)	10	1mM (1mM)	0.15	1E5 (9.77E6)	59.74	100 (9770.79)	59.74
(200; 22)	20	1mM (1mM)	0.21	1E5 (1.17 E7)	98.96	100 (11729.2)	99.01
(200; 16)	60	1mM (1mM)	0.36	1E5 (1.27E7)	92.39	100 (12507.79)	92.30

Online injection first read time 1sec							
Number of : (Ambiguous fits; Outliers)	Read frequency (sec)	Input K_d (Output K_d)	K_d %CV	Input k_{on} (Output k_{on}) $M^{-1}min^{-1}$	k_{on} %CV	Input k_{off} (Output k_{off}) min^{-1}	k_{off} %CV

(0; 0)	1	10pM (10pM)	0.10	1E9 (1E9)	0.12	0.01 (0.01)	0.20
(0; 0)	5	10pM (9.99pM)	2.43	1E9 (1E9)	0.46	0.01 (0.01)	2.81
(0; 0)	10	10pM (10pM)	0.33	1E9 (1E9)	0.37	0.01 (0.01)	0.62
(0; 0)	20	10pM (10pM)	0.43	1E9 (1E9)	0.53	0.01 (0.01)	0.86
(0; 0)	60	10pM (10pM)	0.78	1E9	0.87	0.01 (0.01)	1.46
(0; 0)	1	1nM (1nM)	0.05	1E8 (1E8)	0.46	0.1 (0.1)	0.48
(0; 0)	5	1nM (1nM)	0.12	1E8 (9.99E7)	0.89	0.1 (0.1)	0.93
(0; 0)	10	1nM (1nM)	0.16	1E8 (1E8)	1.36	0.1 (0.1)	1.43
(0; 0)	20	1nM (1nM)	0.25	1E8 (1E8)	1.76	0.1 (0.1)	1.88
(0; 0)	60	1nM (1nM)	0.40	1E8 (9.99E7)	2.91	0.1 (0.1)	3.07
(9; 0)	1	100nM (100nM)	0.05	1E7 (1E7)	3.33	1 (1)	3.35
(58; 0)	5	100nM (100nM)	0.12	1E7 (1.01E7)	8.81	1 (1.01)	8.85
(51; 0)	10	100nM (100nM)	0.17	1E7 (1.01E7)	11.53	1 (1.01)	11.59
(68; 0)	20	100nM (100nM)	0.22	1E7 (1.02E7)	18.16	1 (1.02)	18.24
(77; 0)	60	100nM (100nM)	0.23	1E7 (1.05E7)	17.87	1 (1.05)	17.95
(200; 8)	1	10μM (10μM)	0.05	1E6 (1.16E6)	44.00	10 (11.61)	44.02
(200; 17)	5	10μM (10μM)	0.11	1E6 (1.54E6)	115.22	10 (15.39)	115.24

(200; 52)	10	10µM (10µM)	0.14	1E6 (1.28E6)	247.86	10 (12.84)	248.29
(200; 6)	20	10µM (10µM)	0.22	1E6 (1.08E10)	285.87	10 (1.08E5)	285.94
(200; 16)	60	10µM (10µM)	0.39	1E6 (5.38E9)	252.64	10 (53811.80)	252.71
(200; 13)	1	1mM (1mM)	0.05	1E5 (1.02E7)	55.30	100 (10237.89)	55.30
(200; 14)	5	1mM (1mM)	0.11	1E5 (9.95E6)	55.06	100 (9950.64)	55.05
(200; 16)	10	1mM (1mM)	0.15	1E5 (9.68E6))	49.20	100 (9683.19)	49.20
(200; 8)	20	1mM (1mM)	0.20	1E5 (9.63E6)	55.35	100 (9632.49)	55.33
(200; 16)	60	1mM (1mM)	0.40	1E5 (9.98E6)	60.23	100 (9977.35)	60.20

Supplemental Methods

How to conduct a Monte Carlo Analysis in GraphPad Prism

This analysis will repeat simulations many times, and tabulate selected results. There are essentially 3 steps to follow in order to perform a Monte Carlo analysis:

1. Simulating a data table

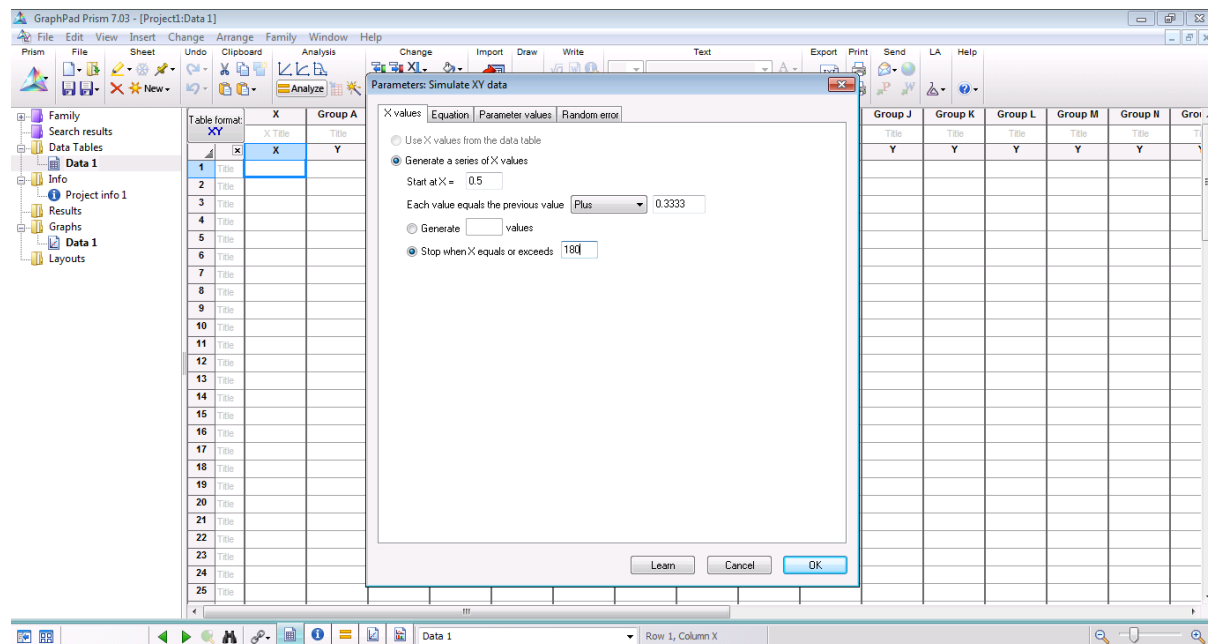
To simulate a family of XY data sets with random error, start from any data table or graph, click **Analyze**, open the **Simulate data** category, and then select **Simulate XY Data**.

X values tab. This allows you to generate a regular series of X values.

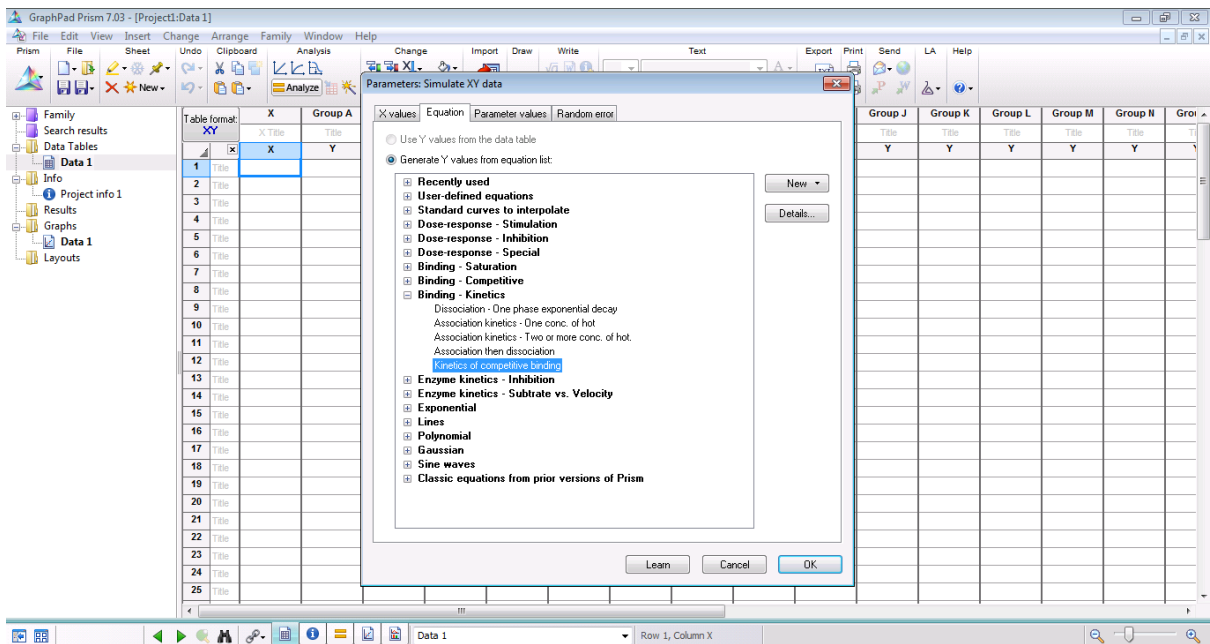
The example described below is performed using the Equation the '**Kinetics of competitive binding**', and forms a small part of our whole analysis.

We chose to simulate X values time (min), using a 30sec start time (i.e. 0.5min, representing offline addition) and generate X values up to 180min, at 20sec intervals (i.e. plus 0.3333min).

These simulations include random scatter, so will produce new results when they are updated.

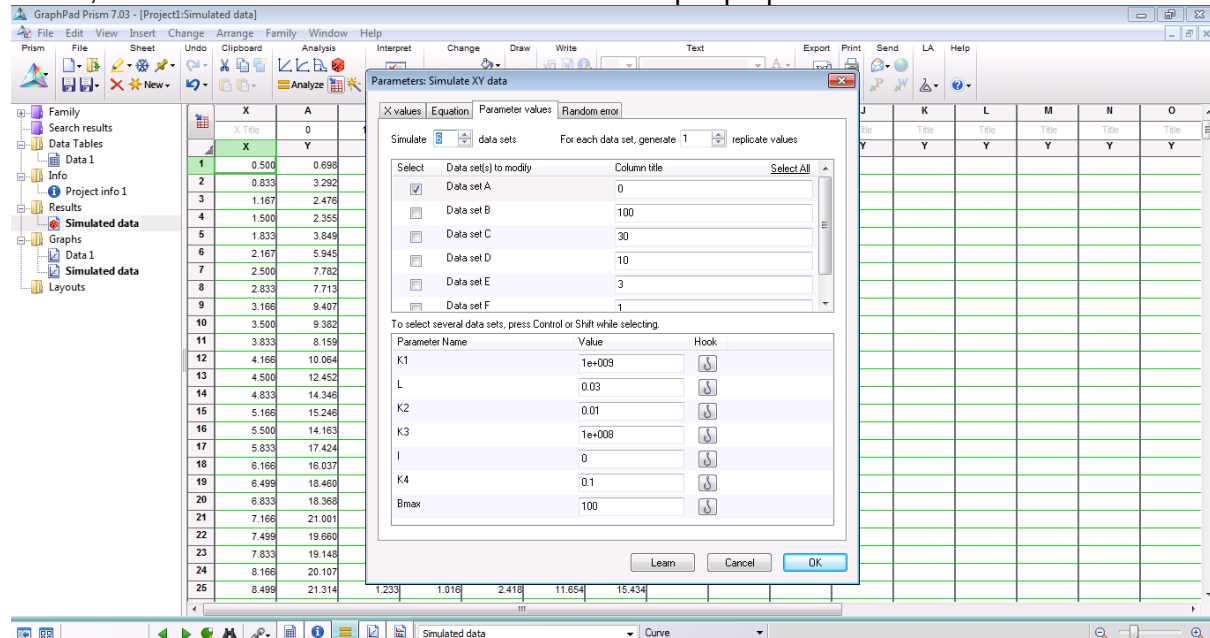


Equation tab. Choose the '**Kinetics of competitive binding**' equation on this tab found listed in '**Binding-Kinetics**' option.



Parameter values tab. On top of the tab, choose how many data sets you wish to simulate, and how many replicates each data set will have.

In this example we chose to simulate using one replicate our tracer ($K_1 = 1 \text{e}9 \text{M}^{-1} \text{min}^{-1}$; $K_2 = 0.01 \text{min}^{-1}$) in the absence of competitor at a concentration (L) $3^* K_d$ (0.03nM), Data set A, column title 0 and our tracer in the presence of a competitor ($K_3 = 1 \text{e}9 \text{M}^{-1} \text{min}^{-1}$, $K_3 0.1 \text{min}^{-1}$), employing five different competitor concentrations (I) ranging from 100 to $1 \text{nM} * K_d$, Data set B to F, column titles 100 to 1. Note for simulation input purposes units are omitted.

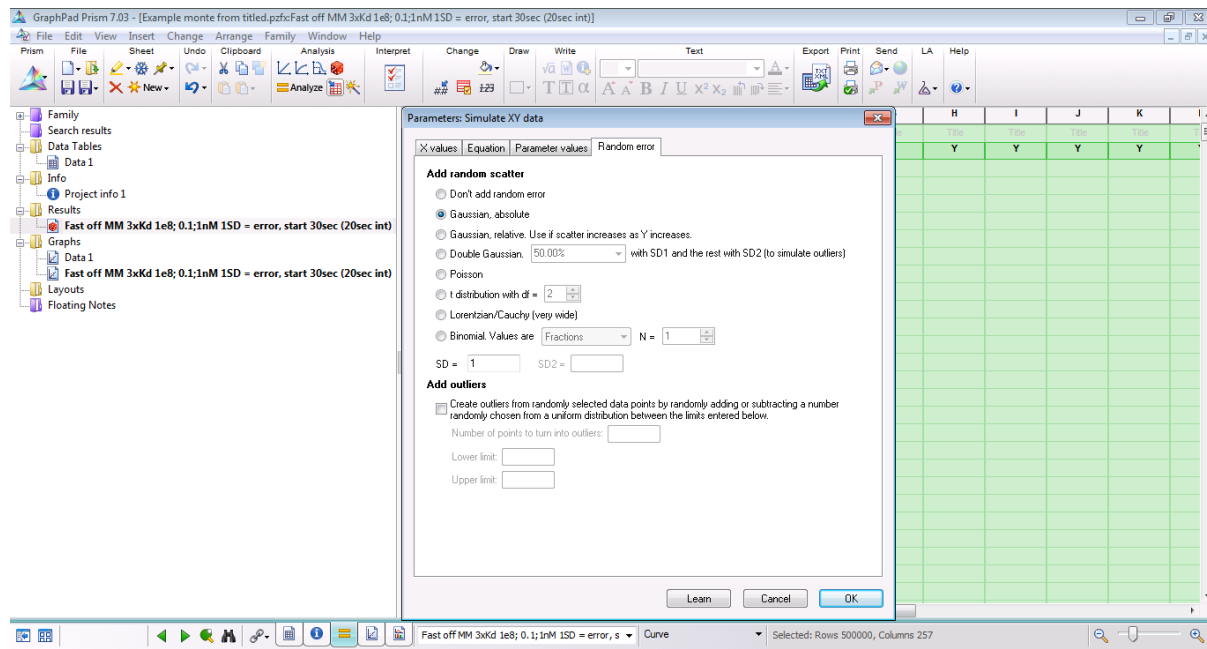


You can choose to simulate multiple data sets (Global fitting), choosing to enter a parameter value for just for one data set (eg. competitor concentrations or I), or to enter a parameter that applies to all data sets, or all, curves (eg. the tracer parameters K_1 , K_2 and L and the competitor parameters K_3 K_4 plus B_{max}).

Random error tab. There are several methods for generating random scatter (and if desired also adding outliers).

GraphPad Prism allows the user to add random error to the generated Y values by taking each theoretical (i.e. ‘correct’) value and adding to it a random number taken from a uniformly distributed population with a standard deviation (SD) defined by the user and equivalent at all concentrations. The random error chosen for simulation was Gaussian absolute to directly reflect the pattern of error observed in our experimental data.

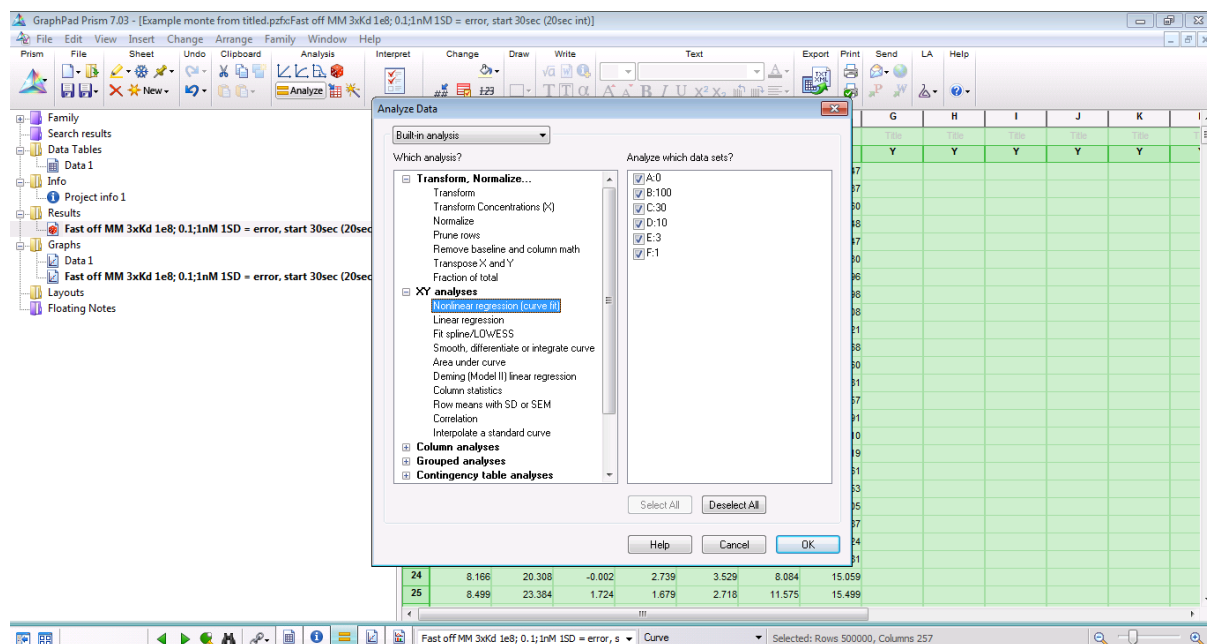
We took the decision to run simulations with minimal error (a standard deviation equal to one) reflecting a high quality assay to test the theoretical limitations of the Motulsky-Mahan model rather than being restricted by what we perceive as technical assay limitations.



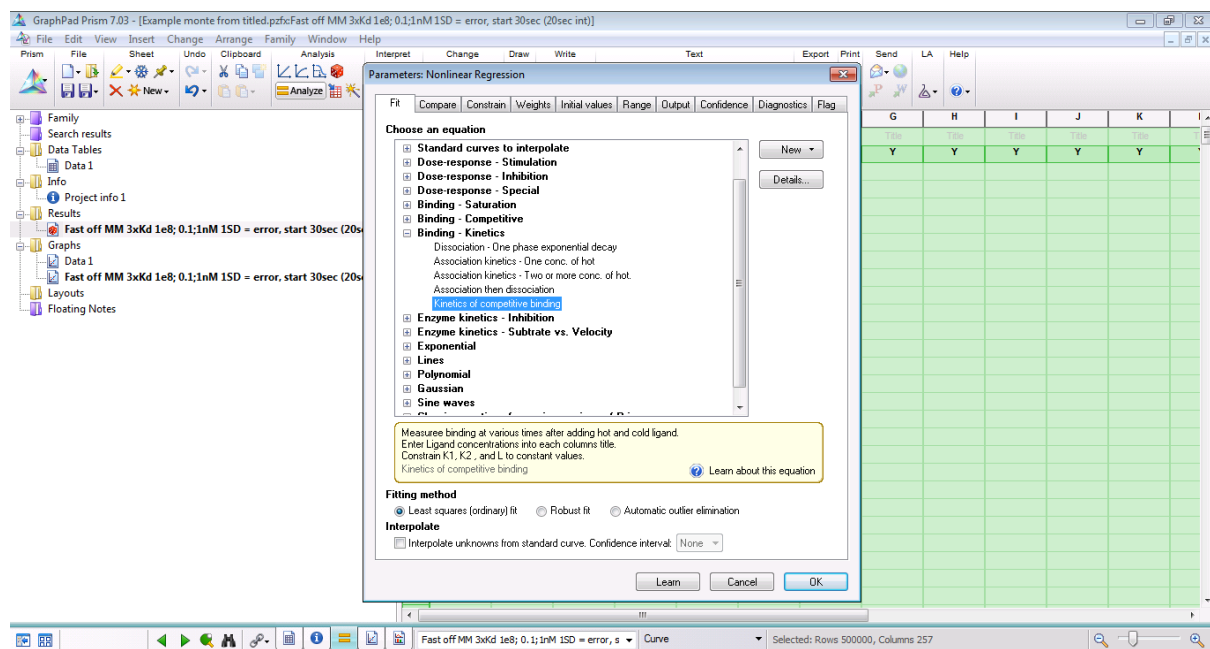
Finally, **title** the ‘simulation’ as you will likely create several varying one or more parameter at a time.

2. Analyze the simulated data set using the equation Kinetics of competitive binding.

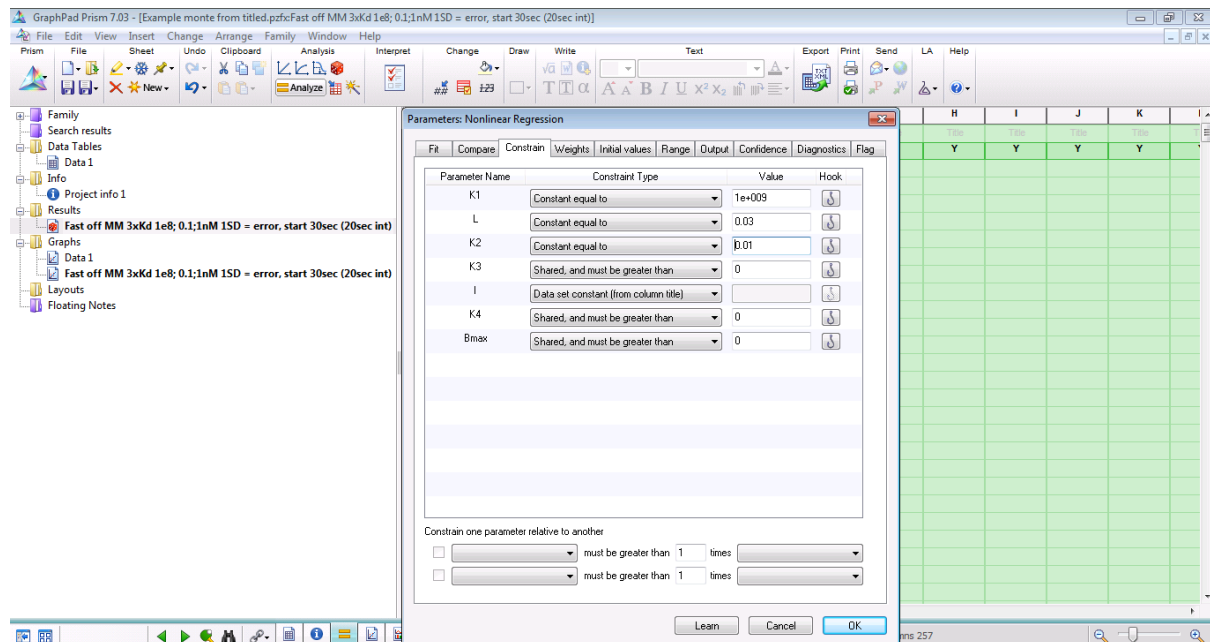
To do this click **Analyse**, and choose **XY analyses (Non-linear regression curve fit)**



Then choose the **Kinetics of competitive binding** equation on this tab found listed in 'Binding-Kinetics' option.

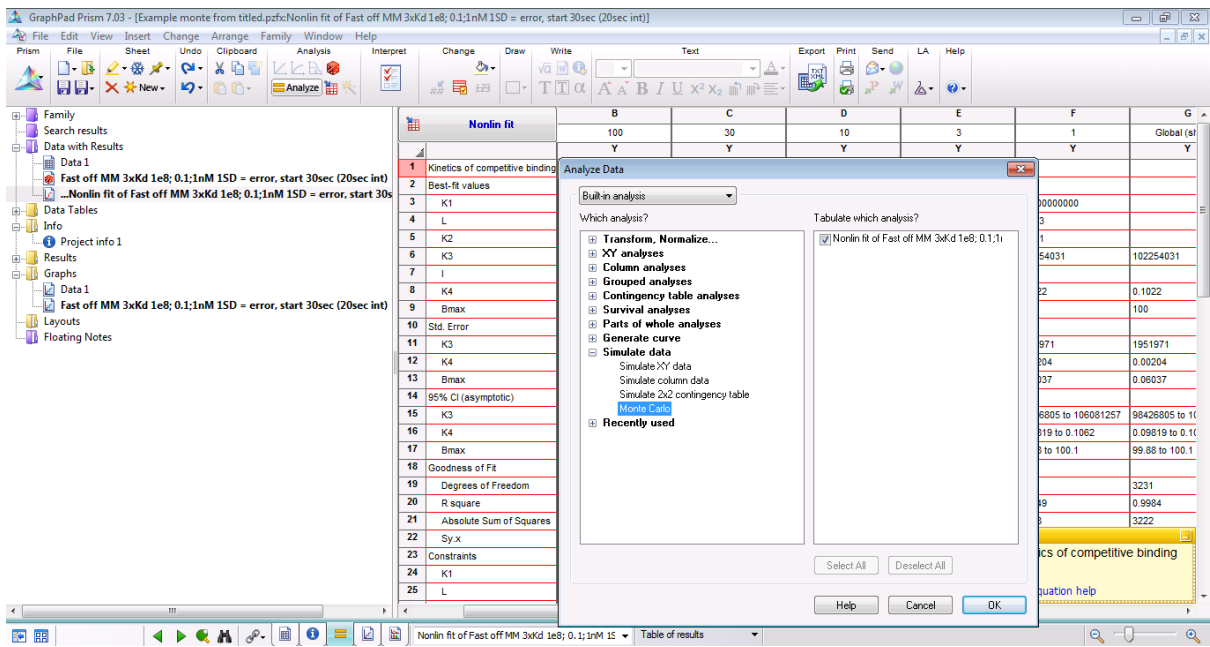


Then click on the **constraint** tab and constrain the parameters of the tracer eg k1, k2 and L, as described above.

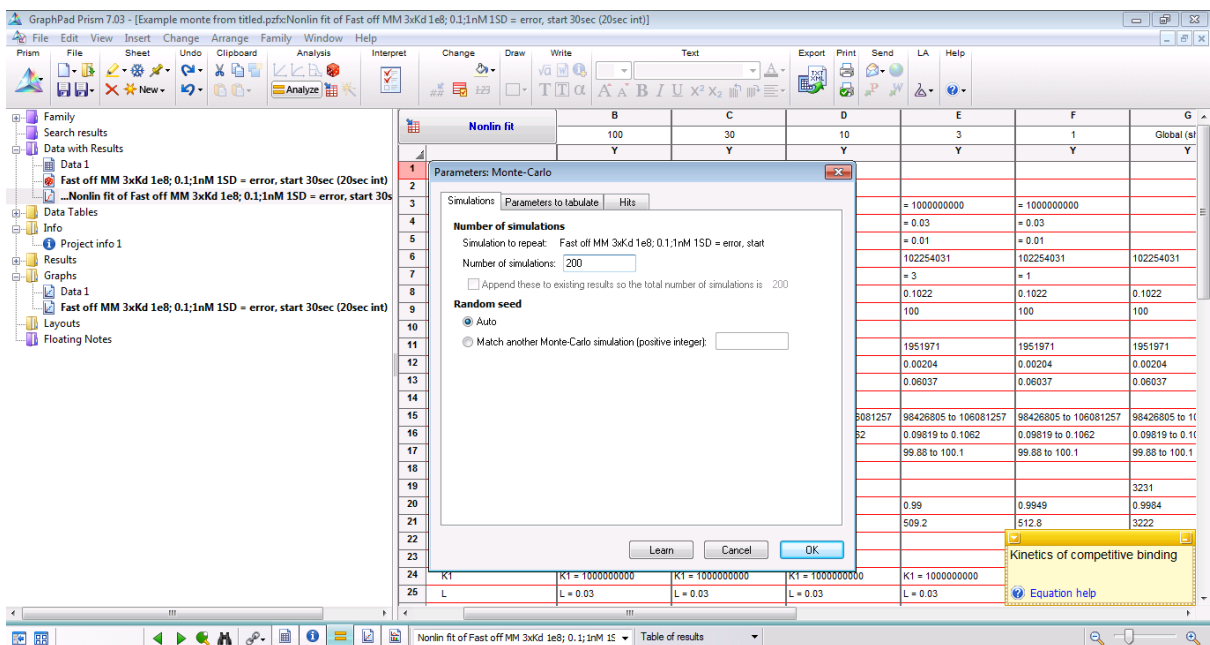


3. Perform the Monte-Carlo analysis.

Start from the nonlinear regression **results page**, click **Analyze** and choose **Monte Carlo** simulation.

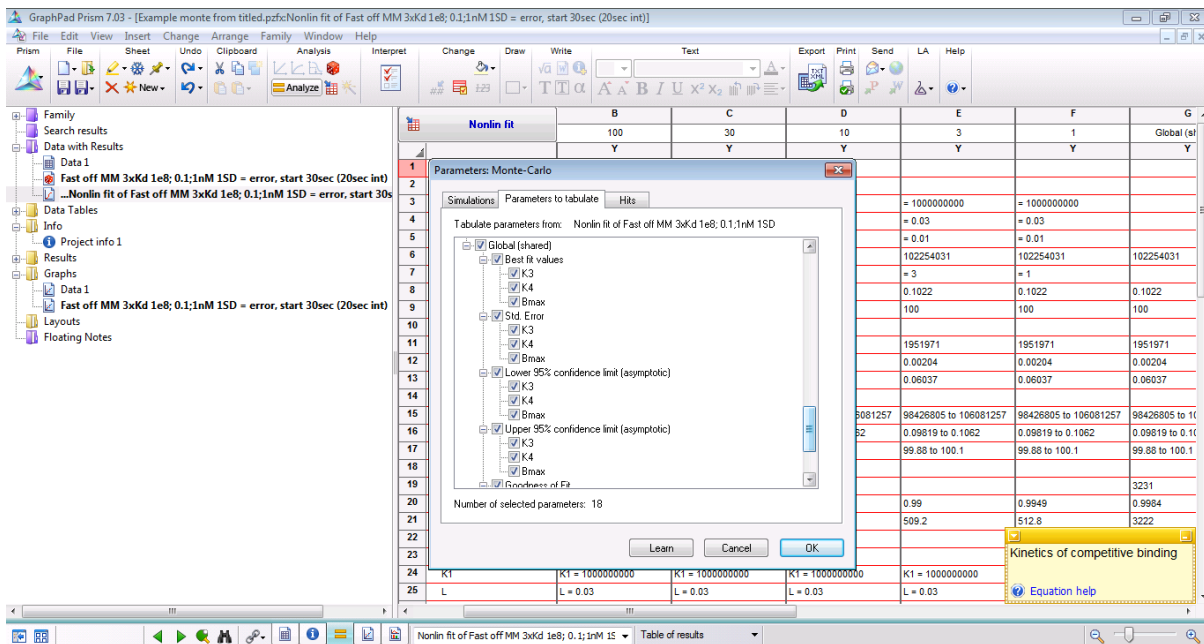


On the first (simulations) tab, choose how many simulations you want Prism to perform. We chose to perform 200 simulations per test condition.

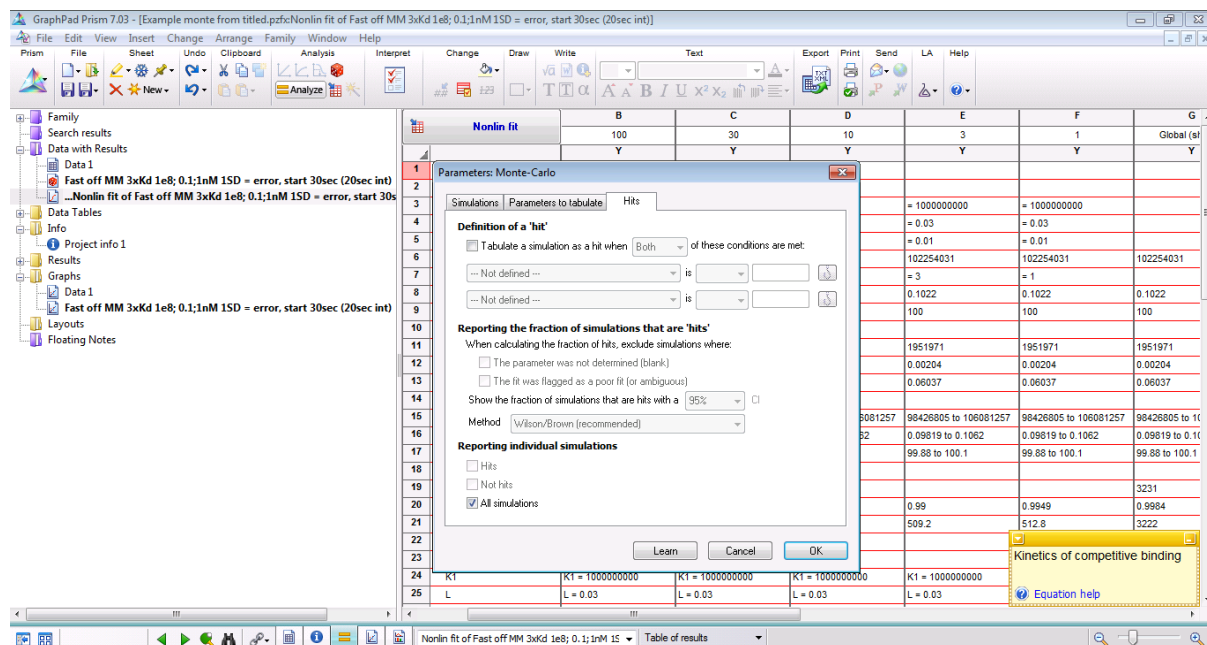


On the **Parameters to tabulate** tab, choose which parameters you want to tabulate. The choice is the list of analysis constants that Prism creates when it analyses the data.

For this example, we chose to tabulate all the **Global (shared) parameters**.



On the **Hits tab**, you can define a criterion which makes a given simulated results a "hit". We copied all the reported data (Parameters to tabulate) to Excel for further analysis and so chose to report all individual simulations.



Full instructions can be found in the online Prism guide found through the following link under Simulating data and Monte Carlo simulations
https://www.graphpad.com/guides/prism/7/user-guide/index.htm?simulating_data.htm

